PHYSICAL REVIEW C VOLUME 43, NUMBER 2 FEBRUARY 1991

Behavior of nuclear projectile fragments produced in collisions of 14.5 A GeV ^{28}Si with Pb and Cu targets

P. B. Price and Y. D. He
Department of Physics, University of California, Berkeley, California 94720
(Received 16 August 1990)

Using CR-39 nuclear track detectors and an automated scanning system, we have studied the behavior of projectile fragments with charges $8 \leq Z_F \leq 13$ produced in interactions of 14.5 A GeV ^{28}Si nuclei with Pb and Cu targets. Both nuclear and electromagnetic spallation contribute to fragmentation of beam nuclei in Pb and Cu. The total charge-changing cross sections of nuclear projectile fragments with $9 \leq Z_F \leq 13$ interacting in Pb are found to be enhanced by 10 to 30% relative to charge-changing cross sections of stable nuclides. The enhancement occurs primarily in interactions with large loss of charge. In Cu the charge-changing cross sections of secondaries show no significant excess. The mean free path of secondary fragments shows no dependence on the distance from the point of origin. This result rules out at 95% confidence level the production of nuclear fragments with interaction cross sections enhanced by a large factor as conjectured by some workers, but the result is consistent with a two-component model in which ~30% of secondary beams are off-stability isotopes with total cross sections enhanced by ~25%. Our measurements of angular distributions of projectile fragments showed that the transverse momentum distributions are similar to those measured at (1–2) A GeV. The charge pickup cross section of 14.5 A GeV Si is measured to be 0.07–1.3 mb in Pb and ≤0.9 mb in Cu, which is of the same order of magnitude as that measured at ~1 A GeV.

I. INTRODUCTION

Our goal in this work was to establish which aspects of high-energy nucleus-nucleus interactions could be investigated using only plastic track detectors, which can measure charge states and trajectories of minimum-ionizing particles with $Z > 6$. This information should then put us in a position to design future experiments combining plastic detectors with nuclear emulsion or electronic detectors. Specifically, we wanted (1) to measure the total and partial fragmentation cross sections of ^{28}Si into nuclear fragments with $Z > 6$ in Cu and Pb targets of various thicknesses in order to evaluate the contribution and importance of electromagnetic spallation at the energy 14.5 A GeV available at the Brookhaven Alternating Gradient Synchrotron (AGS), (2) to study the interaction of secondary fragments produced in collisions of ^{28}Si beam nuclei in the same Pb and Cu targets, in particular, to search for a dependence of the local mean free path of projectile fragments on the distance from the point of formation, which might indicate the production of anomalous fragments, (3) to investigate the angular distribution of fast fragments in order to extract information about transverse momentum, and (4) to measure the charge pickup cross section at 14.5 A GeV, which could be compared with values obtained at lower energies.

The availability of beams of 14.5 A GeV ^{16}O and ^{28}Si at the Brookhaven AGS and of 60 A and 200 A GeV ^{16}O and ^{32}S at the CERN Superproton Synchrotron (SPS) has made it possible to study the fragmentation of heavy ions and the behavior of projectile fragments produced in nucleus-nucleus collisions at energies well beyond those previously available at the Lawrence Berkeley Laboratory Bevalac and at the Dubna heavy-ion accelerator. Two groups[1–3] have independently used CR-39 nuclear track detectors and automated scanning systems to measure the cross sections for fragmentation of 60 and 200 A GeV ^{16}O and ^{32}S at the CERN SPS. Results of the two groups are consistent with each other and can be well reproduced by a theoretical picture in which nuclear fragmentation dominates at small impact parameters and electromagnetic spallation dominates at impact parameters outside the range of the nuclear force. Recently, Brechtmann *et al.*[4] have measured the fragmentation cross section of ^{28}Si in single targets at the Brookhaven AGS and have estimated the contribution of electromagnetic dissociation at 14.5 A GeV. However, no one has yet studied interactions of secondary nuclear beams either at Brookhaven or at CERN.

Our study of interactions of secondary projectile fragments was motivated by observations of higher cross sections of unstable nuclei than of stable nuclei with similar charge at energies below and around ~1 A GeV. Mittig *et al.*[5] have reported that total reaction cross sections at 60 A MeV for neutron-rich nuclei from C to Mg increase linearly with neutron excess at the same fractional rate for all nuclear charges. Tanihata and co-workers[6,7] have found that fragmentation cross sections at ~800 A MeV are greatly enhanced for nuclides near the neutron-drip line (e.g., ^{11}Li) interacting in high-Z targets and have attributed this enhancement at least partly to Coulomb dissociation, as discussed by Hansen and Jonson.[8]

For the investigation of nuclear fragments with an anomalously large fragmentation cross section, our

motivation was the many and conflicting claims of positive results at Bevalac energies.[9] In some experiments it was claimed that some fraction of projectile fragments in nucleus-nucleus collisions at $\sim(1-2)A$ GeV have an effective size that is much larger than that of normal nuclei. These conclusions were inferred from measurements of the local mean free path in nuclear emulsion, which showed that within a few cm from the point of creation, the mean free paths were shorter than those at a large distance.[10,11] The magnitude of this effect was such that it was possible to fit the experimental data with a two-component model in which a few percent of fragments had a mean free path much less than normal. Evidence for the existence of such a phenomenon has been reported sporadically since the 1950's from cosmic-ray experiments.[12] A detailed investigation of this effect was not possible until the early 1980's, when relativistic heavy-ion beams became available at the Bevalac and at Dubna. Despite a number of studies of this phenomenon in beams of $(3.4-4.1)A$ GeV ^{12}C, $2.1A$ GeV ^{16}O, $(3.4-4.1)A$ GeV ^{22}Ne, $1.8A$ GeV ^{40}Ar, $(0.94-1.9)A$ GeV ^{56}Fe, and $1.5A$ GeV ^{84}Kr by different techniques such as track-recording plastic detectors,[13–18] Cerenkov detectors,[19,20] plastic scintillators,[21,22] nuclear emulsions,[23–32] and bubble chambers,[33–36] the situation is still controversial. Particularly, the early nuclear emulsion results were contradicted by other experiments which used different detection methods, and even by other experiments using nuclear emulsion.[23–27] A particularly stringent upper limit on the fraction of anomalous fragments produced in low-Z targets was obtained in two high-statistics electronic experiments[19,20] in which a stack of thin plastic plates was used as both targets and Cerenkov-radiating detectors. Both groups found that nuclear fragments, identified by charge (but not by isotope), had charge-changing cross sections indistinguishable from those of primary beams with the same charge. Some groups have, however, reported evidence for the existence of anomalous fragments with $Z>2$ (Refs. 28–33).

Despite efforts by many groups, the evidence at the Bevalac and at Dubna for the creation of nuclear fragments with anomalously high cross sections for further fragmentation has been weak, unconvincing, and unreproducible, and the entire case may be dismissed as due to fluctuations or systematic error. However, the possibility cannot be completely ruled out that anomalous fragments might be produced only in certain classes of collisions. For example, the conjecture that there is a rather sharp energy threshold for production of fragments with large interaction cross section is supported by recent work of Karev *et al.*,[37] who reported that $\sim 8\%$ of the fragments of $4.5A$ GeV/c ^{24}Mg interacting in plastic Cerenkov-radiating targets have cross sections about a factor of 70 higher than normal. Their results are by far the statistically most convincing evidence for anomalous fragments.

The angular distribution of projectile fragments can be used to infer transverse momenta characteristic of projectile fragmentation at high energies and to search for the onset of new phenomena. Gerbier *et al.*[38] found that the angular distribution of projectile fragments of $200A$ GeV ^{16}O in Pb has a Gaussian shape and that the derived variances of transverse momentum are compatible with those due to Fermi motion in the projectile nucleus, just as was found in earlier work at $\sim 1A$ GeV.[39] An interesting question would be whether the momentum transfer during projectile fragmentation due to electromagnetic dissociation is significantly different from that due to nuclear spallation at the Brookhaven AGS energies.

A number of groups have measured charge pickup cross sections at Bevalac energies for various projectile nuclei in different targets. Ren *et al.*[40] showed that the dependence of the inclusive cross section of the charge pickup reaction on the projectile and target can be described simply by the expression

$$\sigma_{\Delta Z=+1}=1.7\times 10^{-4}\gamma_{PT}A_P^2$$

(in mb), where

$$\gamma_{PT}=A_P^{1/3}+A_T^{1/3}-1.0\ .$$

Possible explanations of this extraordinarily steep A_P^2 dependence at $\sim(1-2)A$ GeV energy region were discussed by the authors. Most of the previous measurements were made at $(1-2)A$ GeV. To explore the underlying dynamics, one must know the energy dependence of the charge pickup cross section. Two groups[41,42] have obtained data for ^{138}La and ^{197}Au down to $\sim 0.5A$ GeV and have found a trend of increasing cross section of charge pickup with decreasing energy in the region near $0.5A$ GeV. A measurement of the cross section at $14.5A$ GeV, an order of magnitude higher than the Bevalac energy, would provide a clue to the physics involved in this process.

In Ref. 43 we gave a brief report on the interaction of secondary nuclei produced in primary collisions of ^{28}Si and Pb targets. In the present paper, we present a much more detailed account of interactions of primary and secondary nuclei with both Pb and Cu targets.

II. EXPERIMENTAL METHOD AND DATA ANALYSIS

Nuclear track-recording plastic sheets of CR-39 ($H_{18}C_{12}O_7$) were used to make high-resolution measurements of the charge of the beam and nuclear fragments. Figure 1 shows the very simple experimental setup for the two exposures. The first stack consisted of four target-detector modules (called D_1, D_2, D_3, and D_4, respectively) preceded by two CR-39 plastic sheets (called D_0). Each module was composed of one 1.6-cm-thick Pb target followed by three sheets of 0.074-cm-thick CR-39 plastic. The second stack consisted of three target-detector modules (D_1, D_2, and D_3), where D_1 and D_3 contained a 1.0-cm-thick Cu target and three CR-39 plastic sheets, respectively, and D_2 contained a 1.6-cm-thick Pb target and three CR-39 sheets. For each module, six surfaces upstream and downstream from the target could be used to identify the charges (but not the masses) of the incoming and outgoing beam particles and projectile fragments. The two sheets in D_0 were used to identify beam nuclei. The two stacks were exposed to a 14.5-GeV/nucleon ^{28}Si beam at a density of about 500 nuclei

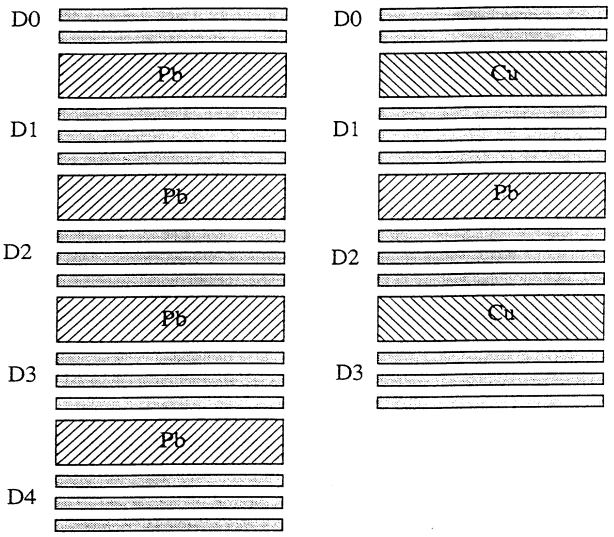

FIG. 1. Experimental setup. (a) Exposure one: four 1.6-cm Pb targets were used. (b) Exposure two: the first and third targets were 1.0-cm Cu; the second target was 1.6-cm Pb.

per cm^2 at normal incidence. After exposure, the plastic sheets were etched in a 6.25 molar NaOH solution (35 and 48 h, respectively, at 70 °C for stacks 1 and 2) to develop conical etchpits at the points of intersection of the trajectories of highly charged particles with the top and bottom surfaces. The techniques are well developed.[44]

A fully automated system was employed to scan all the surfaces of plastic sheets and measure the etchpits due to the beam particles and relativistic nuclear fragments with charges higher than 6 with respect to fiducial beam tracks at two diagonally opposite corners of the sheets. A brief description of this system can be found in Ref. 38. A VAX-750 computer operated X, Y, and Z motors that provided a raster scan in the horizontal plane and kept satisfactory focus on the top surface of a sheet. Focusing was done automatically by interpolation between the stage height Z chosen manually for best focus at a lattice of positions selected before the scan. A charge-coupled device (CCD) viewed the plastic through the optics of a Leitz Metalloplan microscope at a magnification of 10×. A Vicom image processor digitized each field of view, stored the location of the centroid of each etchpit, and measured the perimeter of each etchpit by a gradient operation followed by thresholding and thinning operations. The perimeter was fitted by an ellipse in on-line analysis, providing the parameters of elliptic fit to the etchpit mouth and the coordinates X and Y relative to the fiducial events.

In the off-line data analysis, the following procedures were applied: (1) Slight variations with position of the sensitivity of an individual sheet, typically less than 0.3 charge unit over an entire sheet, were eliminated by dividing a sheet into a 12×12 bin array and scaling the minor axis of all tracks due to beam nuclei in that bin. The resulting distribution of the minor axis of etchpits led to a great improvement in charge resolution. (2) In order to reconstruct the trajectories of events and study the angular distribution of projectile fragments, etchpits on each surface were matched to those on the preceding surface. This step allowed both spallation recoil tracks, whose range was always much less than the thickness of a sheet, and surface flaws which showed up on one surface as a randomly located background, to be rejected. It turned out that matching distances of 50 μm for two surfaces within one module and of 200 μm for two surfaces on the opposite side of the target were reasonable. The mean lateral displacement of tracks passing through a 1.6-cm Pb target and a 1.0-cm Cu target due to multiple Coulomb scattering was estimated to be ~ 10 and ~ 4 μm, respectively, far smaller than both the mean spacing of tracks (~ 450 μm) and the maximum allowed lateral displacement for matching tracks, allowing us to follow the trajectories without any problem. For one set of two adjacent surfaces, there happened to be a systematic deviation in the alignment of as much as ~ 15 μm, which we attributed to astigmatism of the stage position encoders and to dilation of one sheet relative to another due to humidity and temperature changes during the measurement. A linear transformation involving six parameters, as used in the previous study,[38] improved the alignment of events down to a few μm for a single etchpit. A divergent or convergent beam would not have caused a problem, since the dilation was based also on the change of the distance between the two fiducial tracks, which were chosen to be two beam particles. (3) Two cuts on tracks were used: a value of $\chi^2 < 0.6$ for the elliptic fitting of etchpits ruled out most of the surface flaws, and $0.94 <$ major-axis/minor-axis < 1.1 rejected not only surface flaws but also most of the overlapping etchpits due to tracks that crossed in regions where the density of beam particles was unusually high.

In a nuclear track-recording solid such as CR-39, the area or minor axis of the elliptically shaped etchpit mouth is a sensitive function of the quantity Z/β of the particle passing through it, for a range of values of Z/β to which the detector is sensitive ($Z/\beta > 6$ in this experiment). For projectile fragmentation of minimum-ionizing particles ($\beta \sim 1$), the velocity of the nuclear fragment is essentially the same as that of the projectile, as a consequence of which there is a monotonic relation between charge and minor axis of the etchpit due to either the beam nucleus or the nuclear fragment. A simple nonlinear transformation, determined for each surface, converts a distribution of minor axes to a charge distribution. In the fourth and fifth lines of Table I, we list typical values of minor axes of etchpits on the top surface of the first sheet in module D_1 corresponding to different charges for stacks 1 and 2. One notices that the change in minor axis per unit change in charge decreases somewhat with increasing charge, due to the nonlinear relation between etchpit radius and charge, as a consequence of which the charge resolution increases with decreasing charge. The charge resolution resulting from measurements of etchpits on one surface varies from ~ 0.16 to 0.20 charge unit for charge $Z = 8-14$. For each module, measurements of six etchpits per track in three CR-39 plastic sheets leads to a charge resolution of 0.08–0.12 charge unit. As an example of the excellent charge reso-

TABLE I. Beam composition, scanning efficiency for a single surface, and mean size of minor axis of etchpit mouth in CR-39 as a function of fragment charge.

Charge of fragment	6	7	8	9	10	11	12	13	14
Detection efficiency (%)	~0	70	85	92	95	96	96	96	96
Composition of beam (%)	~0	~0	1.28	0.65	1.38	1.56	2.95	3.65	88.5
Minor axis (μm) in stack 1	≤ 8	9.1	10.9	12.2	13.2	14.0	14.7	15.3	15.9
Minor axis (μm) in stack 2	≤ 10	12.8	15.1	16.9	18.3	19.4	20.3	21.2	21.9

lution of our detectors, Fig. 2 shows the correlation between charges of events registered in two adjacent modules D_2 and D_3 of stack 2.

The detection efficiency as a function of charge is essentially unity for particles with charges $Z=9-14$ and decreases to zero as the charge decreases from $Z=9$ to 6. A typical set of data for detection efficiency of a single measurement of etchpits is given in the second line of Table I. By applying an appropriate algorithm to the six measurements taken in each module, we were able to achieve 100% detection efficiency for charges $Z=8-14$. In the third line of Table I we list the composition of the different nuclear species in the beam measured in D_0 module. One sees that a small fraction of the Si nuclei fragmented before impinging on our detectors. In our analysis, we follow only Si nuclei into the stack. Charge-changing reactions are defined by a sudden change of measured charge. Figure 3 displays charge states as a function of depth in the stack for a sample event, in which two charge-changing interactions took place, one in the first ($\Delta Z=-1$) and one in the third ($\Delta Z=-5$) Pb targets.

III. FRAGMENTATION OF 14.5 A GeV IN Pb AND Cu TARGETS

Table II gives the total charge-changing cross sections and partial cross sections for fragmentation of Si ($Z=14$) into nuclei with charge $Z_F=8-13$ in Pb and Cu targets with various thicknesses. The errors include counting uncertainty only. To correct partial cross sections for loss of fragments within the target, we used the expression for cross section in a thick target given by

$$\sigma(^{28}\mathrm{Si},Z_T,Z_F)=N(Z_F,Y)A/N(^{28}\mathrm{Si},y)N_A\rho y\ , \qquad (1)$$

where $N(^{28}\mathrm{Si},y)$ and $N(Z_F,y)$ are the number of surviving ^{28}Si nuclei and of fragments Z_F at depth y, N_A is Avogadro's number, and ρ and A are the density and atomic number of the target. This expression differs from the simple exponential relation for production in a thin target; it is valid for a thick target when the total charge-changing cross sections for ^{28}Si and for Z_F are equal. We showed earlier[1] that even if they differed by as much as 50%, Eq. (1) would be correct to within 10%. For a total cross section in a thick target, the usual exponential absorption equation is valid.

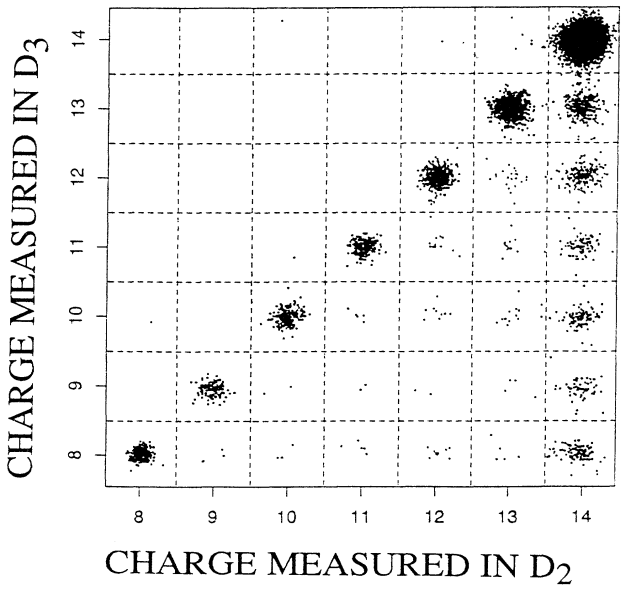

FIG. 2. An example of the correlation between measured charges, for events registered in modules D_2 and D_3 of stack 2. Diagonal elements represent noninteracting primary and secondary beams; off-diagonal elements represent beams that interacted in the second Cu target.

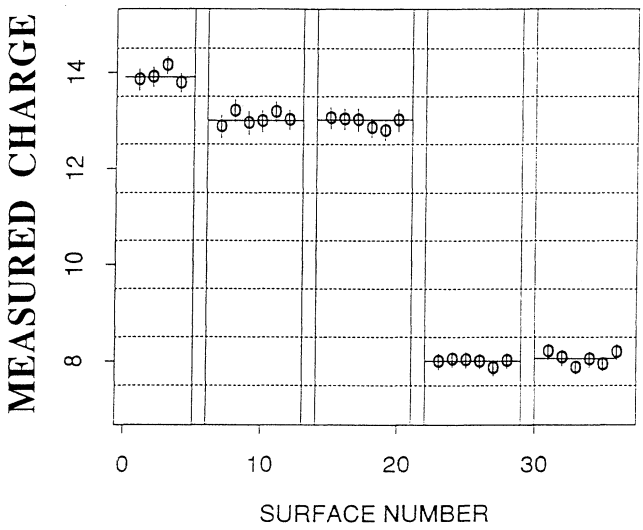

FIG. 3. The charges measured in all surfaces of CR-39 for a sample event with two charge-changing reactions. The charge resolution for a measurement on a single surface varies from 0.16 to 0.20 for charges from 8 to 14. In the plots, the surface number is accounted in such a way that it includes surfaces of target.

TABLE II. Total charge-changing cross sections and partial cross sections for fragmentation of 14.5 A GeV Si into fragments with charge $Z_F = 8-13$ in Pb and Cu targets of various thicknesses. All cross sections are given in mb.

Target	Total	$Z_F=13$	$Z_F=12$	$Z_F=11$	$Z_F=10$	$Z_F=9$	$Z_F=8$	$Z_F \leq 7$
~1-cm Pb[a]	4992±99	1039±41	441±28	125±16	126±15	96±13	138±16	3027±99
First 1.6-cm Pb	5022±66	1072±33	483±22	163±13	155±12	80±9	197±14	2872±66
Second 1.6-cm Pb	5473±80	1078±38	542±27	207±17	190±16	87±11	203±17	3166±80
Third 1.6-cm Pb	5627±95	1199±47	546±31	223±20	248±22	113±15	217±20	3081±95
Fourth 1.6-cm Pb	5631±111	1064±52	605±40	240±25	209±23	106±17	243±25	3164±111
~1-cm Cu[a]	2457±59	288±14	190±11	79±7	81±7	54±6	104±8	1661±59
First 1.0-cm Cu	2464±38	267±14	209±12	96±8	97±8	80±7	135±10	1580±38
Second 1.6-cm Pb	5403±83	1102±40	484±27	224±27	198±17	111±13	222±18	3062±83
Third 1.0-cm Cu	2563±42	328±20	210±16	107±11	120±12	65±9	123±12	1610±42

[a]These data are taken from Ref. 4 for comparison.

In Table II the cross sections of ^{28}Si in single Pb and Cu targets measured by Brechtmann *et al.*[4] are included for comparison with our present data. One sees that our results in the first Pb target of stack 1 and in the first Cu target of stack 2 are consistent with the results of Brechtmann *et al.*[4]

In order to estimate the contribution from electromagnetic dissociation to the measured cross sections in the first target, we have applied the procedures used by Price *et al.*[1] and Brechtmann *et al.*[2–4] We assumed the cross section for electromagnetic dissociation to a fragment Z_F to be the difference between the measured partial cross section to Z_F and the cross section for nuclear fragmentation to Z_F. This approach is based on the assumption that nuclear spallation occurs at impact parameters less than some value R and that electromagnetic spallation occurs at impact parameters greater than R and without interference. As a consequence, the measured overall cross sections are due to a superposition of a series of collisions at different impact parameters. Because the nuclear spallation cross section is essentially energy independent at energies above about 1 A GeV, one could, in principle, obtain electromagnetic spallation cross sections at a given high energy by simply subtracting the spallation cross section measured at relatively low energy, say, 1 A GeV, where electromagnetic spallation is negligible, at least for targets with not too high Z. Unfortunately, fragmentation cross sections for ^{28}Si are not available. Therefore, for nuclear spallation (NS) we used the semiempirical expression of Westfall *et al.*,[45] which fitted data obtained at (1–2) A GeV for projectiles and targets of mass $A_P > 12$ and $A_T > 12$:

$$\sigma_{\rm NS}(P,T) = \pi r_0^2 (A_P^{1/3} + A_T^{1/3} - b)^2 ,$$

where $r_0 = 1.35$ fm and $b = 0.83$, to calculate the nuclear fragmentation contribution to the total charge-changing cross section. The results are compatible either with that obtained by interpolation of fragmentation cross sections for various nuclei measured at Bevalac energies[46] or with that calculated by Karol's soft-spheres model[47] within errors of 3%. The electromagnetic spallation cross sections constitute ~24 and ~10% of the total charge-changing cross sections in Pb and Cu targets, respectively.

For partial cross sections of fragmentation into various fragments, a factorization is valid not only for nuclear spallation but also for electromagnetic dissociation (ED), and therefore the measured cross section can be expressed by the following formula:

$$\sigma(P,T,F) = \sigma_{\rm NS}(P,T,F) + \sigma_{\rm ED}(P,T,F)$$
$$= \gamma_{PF}\gamma_T + \varepsilon_{PF}\varepsilon_T ,$$

where γ_{PF} and ε_{PF} depend on projectile and fragment, whereas γ_T and ε_T depend on only projectile and target. Adopting the γ_T and ε_T obtained in Ref. 4, we have estimated the $\sigma_{\rm NS}(P,T,F)$ and $\sigma_{\rm ED}(P,T,F)$ in the first Pb target of stack 1 and the first Cu target of stack 2. The derived nuclear spallation and electromagnetic dissociation cross sections shown in Fig. 4 confirm the results of detailed work in which Brechtmann *et al.*[4] showed that the measured $\sigma_{\rm ED}$ is consistent with a calculation by the virtual photon method[48] using experimental measurements of photonuclear cross sections. We emphasize that electromagnetic dissociation plays a very important role in fragmentation involving small charge loss. For instance,

$$\sigma_{\rm ED}(\Delta Z = 1) \sim 5\sigma_{\rm NS}(\Delta Z = 1)$$

in Pb and

$$\sigma_{\rm ED}(\Delta Z = 1) \sim \sigma_{\rm NS}(\Delta Z = 1)$$

in Cu at 14.5 A GeV. However, $\sigma_{\rm ED}(P,T,F)$ decreases much more rapidly than $\sigma_{\rm NS}(P,T,F)$ with increasing ΔZ, as seen in Fig. 4. As a way of quantifying the rate of decrease of the cross section with ΔZ, we fitted the data in Fig. 4 to exponentials for values of ΔZ from 1 to 5. The indices are -1.10 for $\sigma_{\rm ED}$ and -0.22 for $\sigma_{\rm NS}$. For $\Delta Z = 6$, 7, and 8 (Ref. 4), the cross sections change irregularly and much less rapidly than exponentially.

A major new result of the present work is that both the total charge-changing cross section and the partial cross sections in a particular Pb target increase monotonically with the thickness of Pb target previously traversed (see Table II). For the total cross section in Pb targets, the increase is ~13% over the range of thicknesses studied (~5 cm in Pb); for some of the partial cross sections, the

percent increase is much larger. Figure 5 shows the total and partial cross sections measured in stack 1 as a function of depth in the stack. Both the total and partial cross sections are seen to depend weakly on the thickness of target previously traversed, with different exponential indices for different reaction channels.

The simplest explanation for these increased cross sections for charge loss of Si, and the one we consider first, would be that neutron removal reactions convert a considerable fraction of the ^{28}Si nuclei to lighter isotopes, which probably have higher fragmentation cross sections than ^{28}Si does and are not distinguishable from ^{28}Si in our detectors. A recent measurement[49] of exclusive cross sections for projectile reactions $^{28}\text{Si}\rightarrow n+^{27}\text{Si}$ and $^{28}\text{Si}\rightarrow 2n+^{26}\text{Si}$ in a thin Pb target gave $\sim$570 and $\sim$95 mb, respectively, of which 264 and 3 mb were due to electromagnetic dissociation and the remainder were due to nuclear spallation. Using these cross sections, the 13% increase of $\sigma_{\Delta Z}$ with Pb thickness given in Table II and Fig. 5 could be quantitatively accounted for if $\sigma_{\Delta Z}$ of the light isotopes of Si were nearly three times as large as that of ^{28}Si. Alternatively, if the cross section for all neutron-removal processes with $\Delta Z=0$ were higher than for $1n$ and $2n$ alone, $\sigma_{\Delta Z}$ for the light isotopes of Si could be less than three times as large as for ^{28}Si. There exist cases in which cross sections for fragmentation of unstable nuclides are greatly enhanced. For example, cross sections for electromagnetic spallation of ^{11}Li and ^{14}Be in Pb are 40 and 80 times larger than that for ^{12}C in Pb after scaling the cross section by Z_P^2 (Ref. 6). Another conceivable alternative is that an excited state of ^{28}Si is responsible for the larger cross section. If so, a fit to our data constrains its proper lifetime to be greater than $\tau\sim 10^{-10}$ sec.

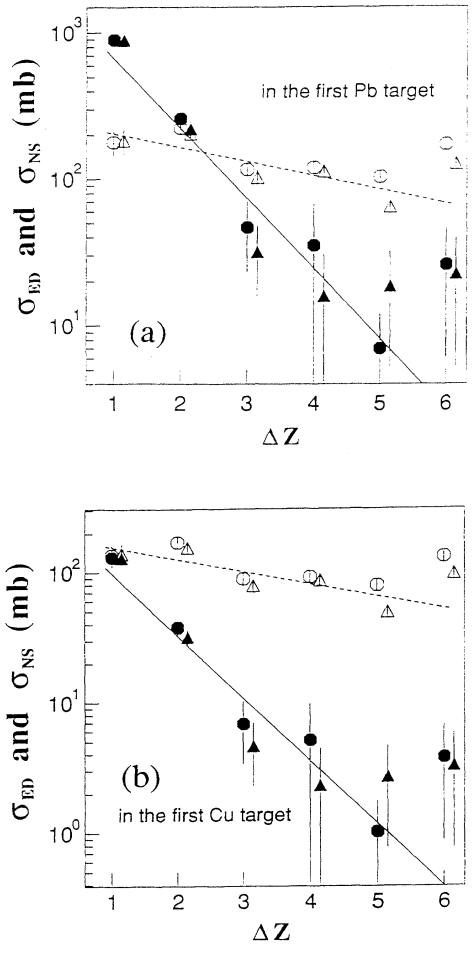

FIG. 4. The partial nuclear spallation cross section $\sigma_{NS}(Z_P,T,Z_F)$ and electromagnetic dissociation cross section $\sigma_{ED}(Z_P,T,Z_F)$ for $\Delta Z(\equiv Z_P-Z_F)=1$–6. The $\sigma_{NS}(Z_P,T,Z_F)$ is represented by open symbols and $\sigma_{ED}(Z_P,T,Z_F)$ by solid ones. The data are compared with the work of Brechtmann *et al.* (Ref. 4) (shown by triangles) and fitted by an exponential function with exclusion of $\Delta Z=6$ (shown by the dashed lines). (a) Results for the first Pb target of stack 1; (b) results for the first Cu target of stack 2.

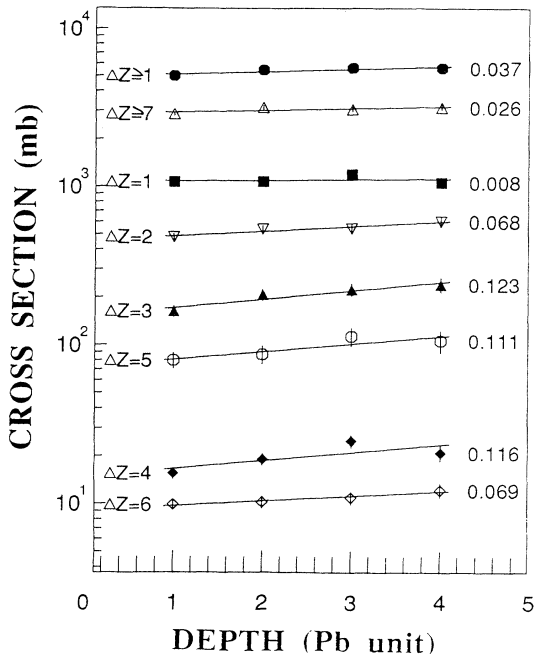

FIG. 5. The cross section $\sigma(Z_P,\text{Pb},Z_F)$ for fragmentation with charge change $\Delta Z(\equiv Z_F-Z_P)\geq 1$, $\Delta Z=1$–6, and $\Delta Z\geq 7$ as a function of depth in the stack. The data for $\Delta Z=4$ and 6 have been multiplied by factors of 0.1 and 0.05 in order to show them clearly. The numbers marked on each line are indices of exponential fit to the data.

IV. INTERACTIONS OF PROJECTILE FRAGMENTS WITH CHARGES $8\leq Z\leq 14$

Figure 6 shows our data for total charge-changing cross sections and for one-charge-loss cross sections for secondary projectile fragments with charges from 8 to 13 and for nuclei with $Z=14$ (^{28}Si + lighter isotopes of Si).

Instead of plotting absolute cross sections, we have chosen to plot an enhancement of the cross section relative to that expected for nuclei on the stability line. We must explain how we chose the cross sections for primary nuclei. For ^{28}Si we used the data of Brechtmann *et al.*[4] For ^{16}O, since no measurement at 14.5 A GeV exists, we used a logarithmic energy interpolation between the values at high energies (60 and 200 A GeV) (Ref. 2) and at 2.1 A GeV.[46] We assumed, for definiteness, that the total fragmentation cross sections of primary nuclei from 9 to 13 lie on a linear interpolation between the values for ^{16}O and ^{28}Si, and we plotted in Fig. 6 the percentage difference between our measured cross section and this linear interpolation. We note that almost all the cross sections of secondary nuclei are enhanced compared to those of primary nuclei with the same charge.

We first discuss the data in Pb targets, drawing attention to three features: (1) Secondary beams of even-Z nuclei have total charge-changing cross sections $\sigma_{\Delta Z\geq 1}$ that are 10–15 % higher than expected for stable nuclei. (2) Secondary beams of odd-Z nuclei have 5–20 % higher values of $\sigma_{\Delta Z\geq 1}$ than do neighboring even-Z nuclei. Therefore, if *primary* beams of odd-Z nuclei were to have $\sigma_{\Delta Z\geq 1}\sim 5$–10 % higher than $\sigma_{\Delta Z\geq 1}$ for *primary* even-Z nuclei, the enhancement for *secondaries* relative to *primaries* would be ~10% for both even and odd species. (3) Interactions involving the loss of one unit of charge [see Fig. 6(b)] are not enhanced enough to account entire-

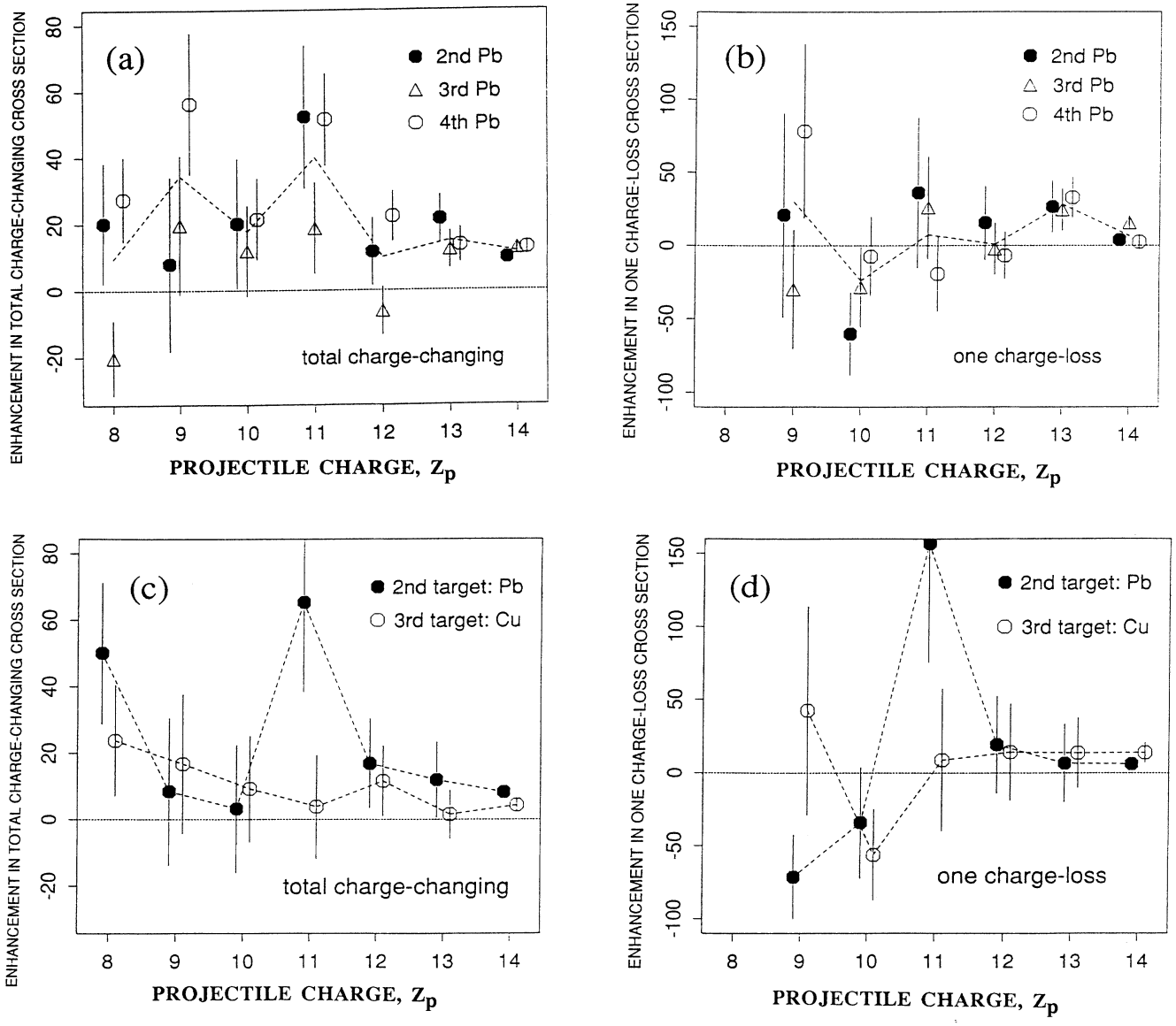

FIG. 6. Percentage enhancement in $\sigma_{\Delta Z\geq 1}$ [(a) and (c)] and in $\sigma_{\Delta Z=1}$ [(b) and (d)] of secondary beams over expected cross sections for primary beams in Pb [(a) and (b)] and Cu [(c) and (d)]. The dashed line connects mean measured values.

ly for the increase in $\sigma_{\Delta Z \geq 1}$, from which we infer that the excess in the total charge-changing cross section is mainly contributed by processes with larger charge loss.

For the Cu data [Fig. 6(c) and (d)], with poorer statistics than for the Pb data, there is weak evidence for an excess in the total charge-changing cross sections but no evidence for enhancement of the one-charge-loss cross sections. (The apparent large excess at $Z_P = 11$ may be a fluctuation.)

Figure 7 shows $\sigma_{\Delta Z}$ of secondary nuclei with $\Delta Z = 1-6$ for Si, 1–5 for Al, 1–4 for Mg, 1–3 for Na, 1–2 for Ne, and 1 for F in various targets. For comparison, the dashed line shows the data for primary ^{28}Si. No data for the partial cross sections of primary beams of F to Al at these energies exist.

To explore further the global total charge-changing

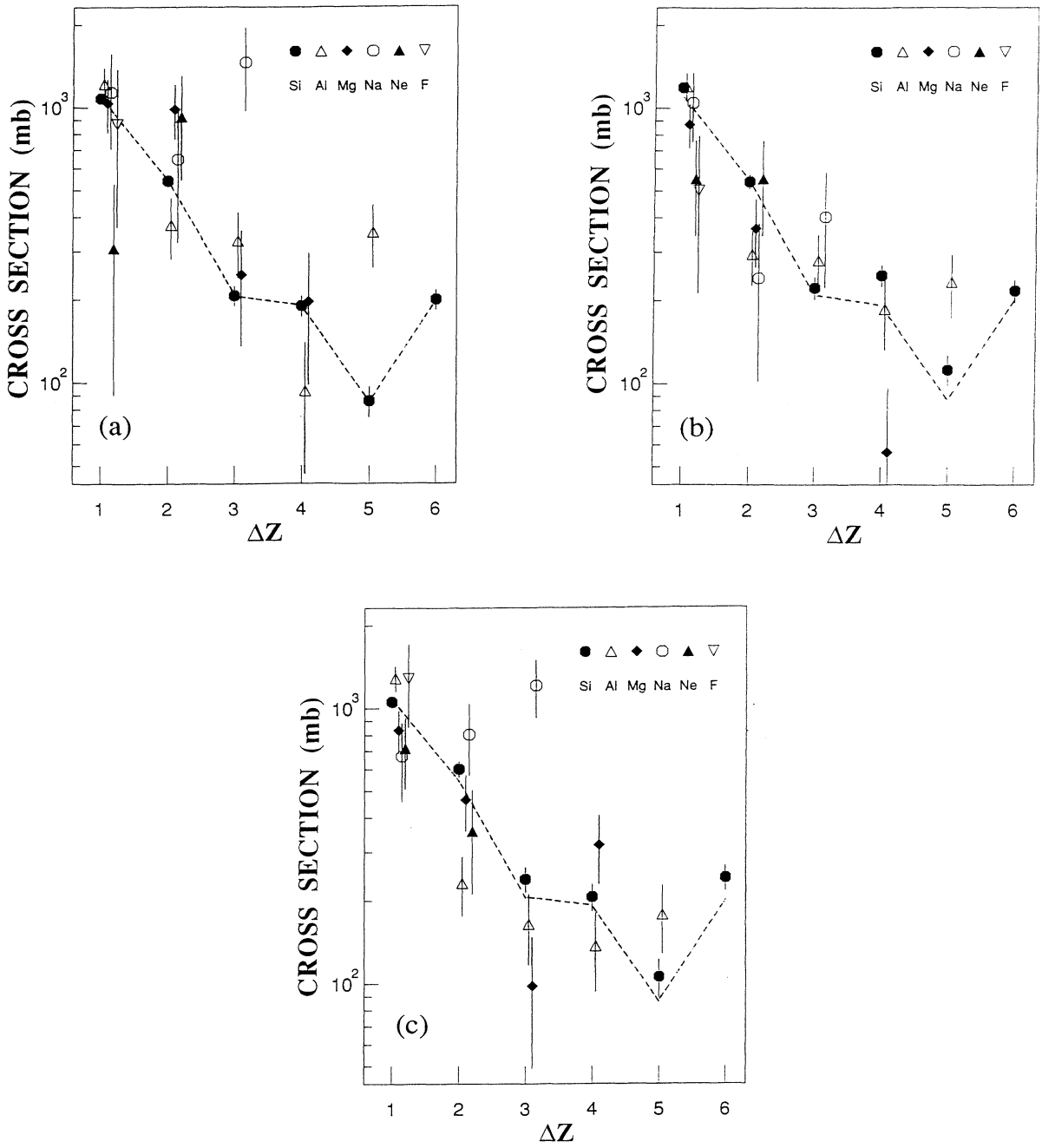

FIG. 7. The partial cross section $\sigma_{\Delta Z}$ of secondary nuclei with $\Delta Z (\equiv Z_P - Z_F) = 1-6$ for Si, 1–5 for Al, 1–4 for Mg, 1–3 for Na, 1–2 for Ne, and 1 for F in the (a) second, (b) third, and (c) fourth Pb targets of stack 1 and the (d) second Pb and (e) third Cu target of stack 2. In all plots, the dashed line connects the partial cross sections of primary ^{28}Si measured in the first Pb target of stack 1 and the first Cu target of stack 2.

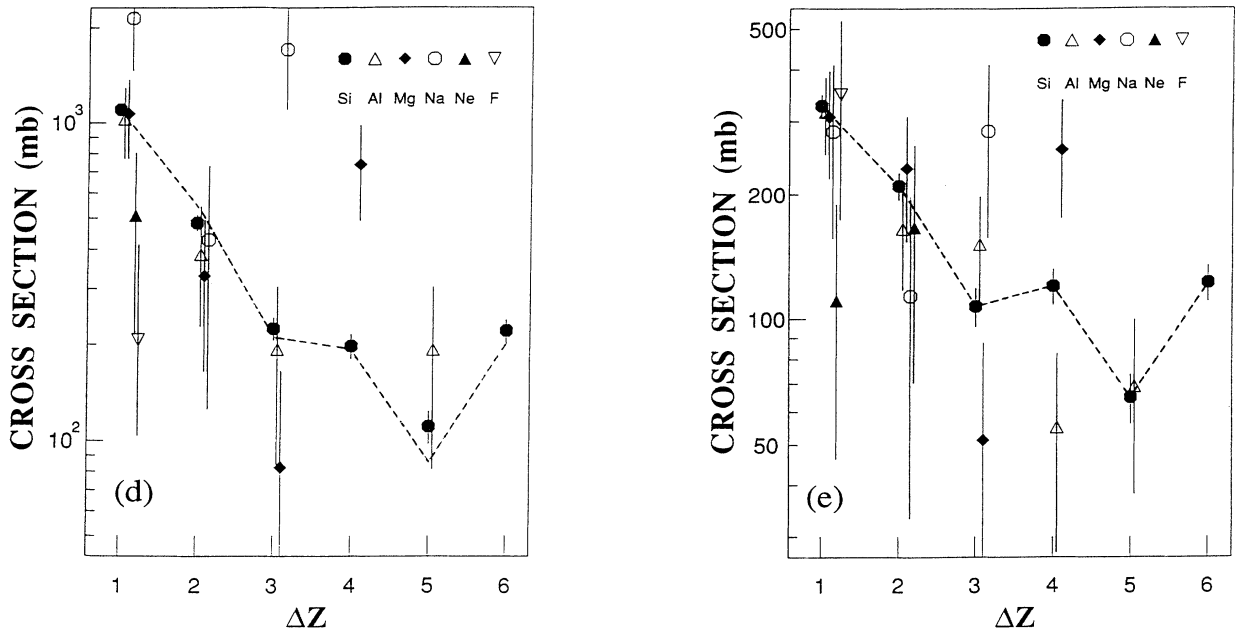

FIG. 7. (*Continued*).

cross sections of secondary beams, and to search for anomalous nuclear fragments, it is useful to organize the data in such a way that one can see the dependence of the mean free path for charge-changing interactions of secondary fragments on the distance from the point of their formation. Figure 8 presents these data for each of the individual nuclear fragments with charge $8 \leq Z \leq 14$. Only statistical counting errors are included in the error bars, and where not shown, error bars are smaller than the size of the points. On such a graph the presence of an admixture of anomalous fragments would be inferred if there were a significantly depressed value of mean free path in the first one or two bins. Figure 9 shows the results of a Monte Carlo calculation for a two-component model in which there are a fraction f of anomalous fragments with mean free path $\lambda_a = r\lambda_n$ and a fraction $(1-f)$ of normal nuclei with mean free path λ_n. Clearly, the typical values of the two parameters for anomalous fragments reported by previous workers ($f = 5-10\%$ and $r = 0.01-0.1$) should yield a significantly depressed mean free path in the first bin. Therefore, the absence of systematically depressed values of mean free path in the first bins of Fig. 8 enables us to set a stringent limit on the presence of an admixture of anomalous fragments. The fitting to our data excludes the region in parameter space of f and r at 95% confidence level shown by the shaded region in Fig. 10. A fraction of 3% or more of anomalous fragments with $r < 0.2$ can be ruled out at 95% confidence level. Our result thus excludes the anomalous fragments with $f = 8.4\%$ and $r = 0.0143$ reported by Karev *et al.*[37] as well as values of f and r inferred from other experiments in which positive claims for anomalous fragments were made. The dashed curve in this figure shows values of f and r that can give rise to a 10% enhancement in total charge-changing cross sections for interactions in each individual module. There do exist values of f and r that can account for the data in both Figs. 6 and 8. Values such as $f = 30\%$ and $r = 0.75$ seem reasonable for the production of unstable isotopes with moderately enhanced fragmentation cross sections relative to stable isotopes.

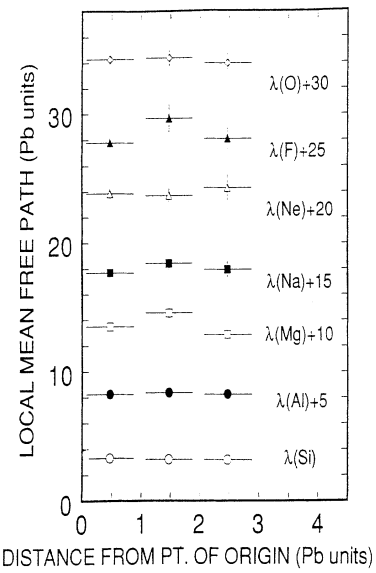

FIG. 8. The local mean free path as a function of distance downstream in Pb units (1 Pb unit = 1.6 cm of Pb + 0.22 cm of CR-39 plastic) from the point of creation. To display all data for different nuclear fragments in the same graph, the measured $\lambda(Z_P)$ have been displaced upward by the number of Pb units indicated.

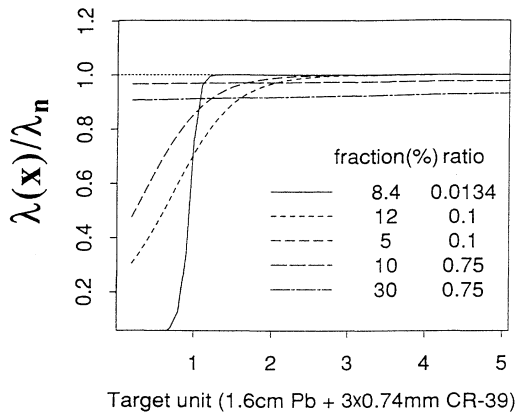

FIG. 9. Dependence of the local mean free path of nuclear species on distance from the point of origin predicted in a Monte Carlo calculation using a two-component model in which a fraction f of nuclei has abnormal mean free path $\lambda_a = r\lambda_n$.

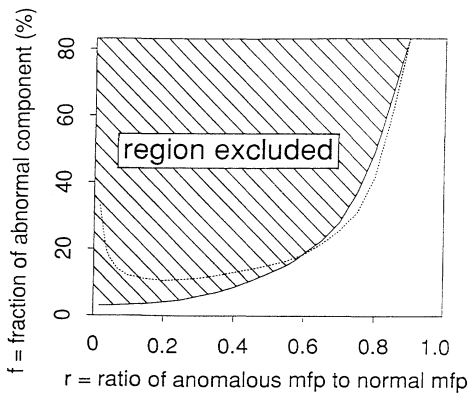

FIG. 10. Values of f and r in a two-component model for enhanced cross sections. The shaded region is excluded by data in Fig. 8. The dashed curve accounts for 10% overall enhancements in $\sigma_{\Delta Z \geq 1}$ given in Fig. 6. There exist values of f and r that can explain the data in both Figs. 6 and 8.

V. ANGULAR DISTRIBUTIONS AND INFORMATION ABOUT TRANSVERSE MOMENTUM OF FRAGMENTS

For a thick-target experiment, with an error in position measurement of a few μm, it is possible to measure the emission angle of projectile fragments in nucleus-nucleus collisions with an accuracy ~ 0.1 mrad. Figure 11 shows the experimental angular distribution for various fragments produced in the first Pb target of stack 1 and in the first Cu target of stack 2. Gaussian fits to the data yield acceptable values of χ^2 for every fragment charge in both targets. The first three rows of entries in Table III give χ^2 per degree of freedom, mean angle $\langle\theta\rangle$, and angular variance σ_θ. A systematic increase of σ_θ with a decrease in fragment charge is seen for both the Cu and Pb targets.

In addition to the finite angular resolution of our detectors, there are two processes which contribute to the angular distribution: multiple Coulomb scattering and momentum transfer in projectile fragmentation. The observed angular distribution is a result of the convolution of three Gaussian distributions due to these three processes. To infer the angular variance due to momentum transfer alone, we carried out a two-step deconvolution operation, the results of which are given in the lower rows of Table III. First, we give the standard deviations after correction solely for finite angular resolution, which varies from sheet to sheet but should be independent of fragment charge. For fragments with charge $Z=14$, although lighter isotopes are produced by neutron knockout reactions, the uninteracted isotope $A=28$ is still dominant ($\geq 70\%$ of charge 14). It is thus reasonable to assume that the standard deviation σ_θ of charge $Z=14$ after correction for angular resolution is due mainly to multiple Coulomb scattering as the first order of approximation. This assumption and the fact that the

TABLE III. Angular distribution parameter and transverse momentum of projectile fragments produced in collisions of 14.5 A GeV ^{28}Si beam with the first 1.6 cm Pb in stack 1 and the first 1.0 cm Cu in stack 2.

Fragment charge	Target	14	13	12	11	10	9	8
χ^2/DOF for	Pb	1.1840	1.1212	1.7535	1.1736	0.7414	1.5074	0.8553
Gaussian fit	Cu	3.2912	0.6004	1.0699	1.0351	0.6549	1.6616	1.1306
Average angle	Pb	0.7777	0.8353	0.9500	0.9595	0.9110	1.0269	1.0992
$\langle\theta\rangle$ (mrad)	Cu	0.9034	0.9449	0.9264	1.0331	1.1613	1.1854	1.1276
Standard deviation	Pb	0.6205	0.6665	0.7580	0.7656	0.7269	0.8193	0.8770
σ_θ (mrad)	Cu	0.7208	0.7539	0.7392	0.8243	0.9266	0.9459	0.8997
σ_θ after correction	Pb	0.5915	0.6395	0.7344	0.7422	0.7023	0.7976	0.8568
for resolution	Cu	0.3994	0.4565	0.4317	0.5652	0.7061	0.7312	0.6704
σ_θ due to	Pb	~ 0	0.2431	0.4352	0.4483	0.3785	0.5350	0.6198
variance in P_T	Cu	~ 0	0.2210	0.1637	0.3999	0.5823	0.6124	0.5384
σ_{P_T} (MeV/c)	Pb	~ 0	92	152	143	110	140	163
(if $A/Z=2$)	Cu	~ 0	84	57	128	169	160	125

multiple Coulomb scattering width depends only on $Z/P\beta$, and thus is a function of the ratio A/Z, allows us to subtract the contribution of multiple Coulomb scattering to angular variance for all the secondary fragments by using the value for $Z=14$. The next to last sets of entries in Table III are the derived net angular variance σ_θ due only to the momentum transfer in projectile fragmentation. The corresponding widths in terms of transverse momentum σ_{P_T} for each fragment are given in the last sets of entries. The errors in measurement of σ_{P_T} are estimated to be ~ 20 and ~ 30 MeV/c for the Pb and Cu targets, respectively.

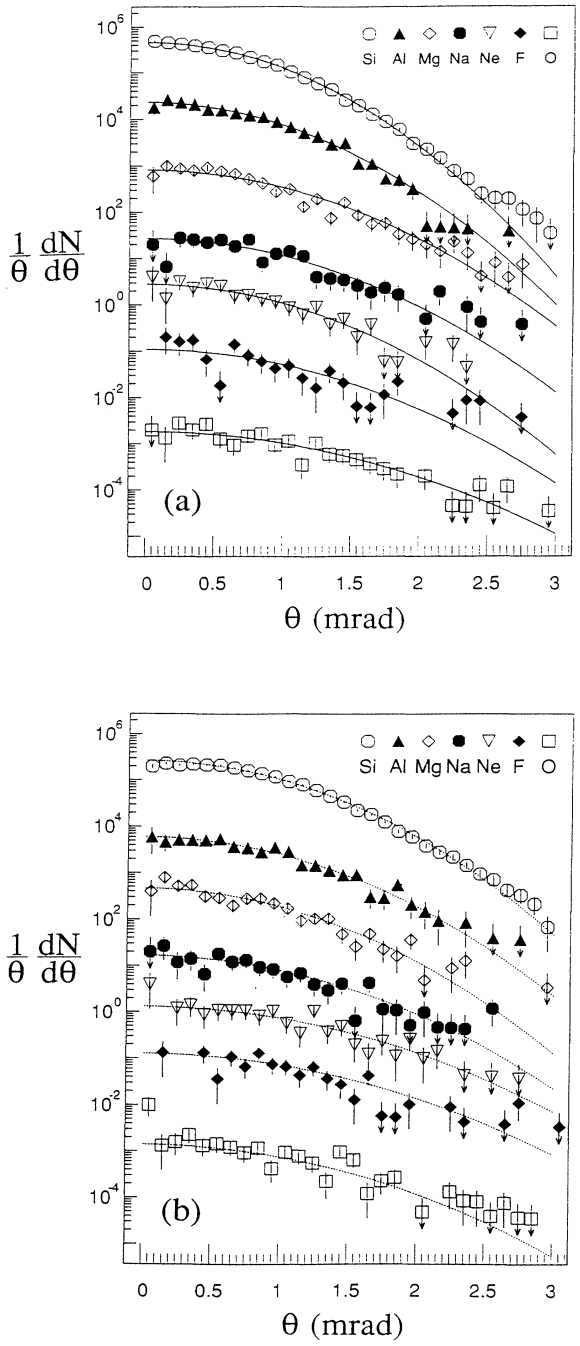

FIG. 11. Angular distribution of various detectable nuclei ($Z=8-14$) produced in (a) the first Pb target of stack 1 and (b) in the first Cu target in stack 2. The data are scaled by factors of 1, 1, 10, 10^2, 10^3, 10^4, and 10^6 for Si, Al, Mg, Na, Ne, F, and O, respectively, in order to display all the distributions in one figure. For χ^2 of fit, average angle $\langle\theta\rangle$, and σ_θ, see Table III.

An earlier study of ^{12}C and ^{16}O at Bevalac energies[39] showed that σ_P depends only on fragment and projectile, not on the target or the beam energy [at least in the energy interval studied, $(1-2)A$ GeV]. A recent measurement of σ_P for fragments C, N, and O in fragmentation of $200A$ GeV ^{16}O in Pb by Gerbier *et al.*[38] confirmed the independence of σ_P on energy in the region of $(1-200)A$ GeV for ^{16}O. A parabolic dependence of σ_P^2 on fragment mass based on Fermi motion was proposed by many authors[50] and was shown by Greiner *et al.*[39] to give a plausible fit to their data on fragmentation of 1.05 and $2.1A$ GeV ^{12}C and $2.1A$ GeV ^{16}O. Figure 12 shows a fit of

$$\sigma_P^2=4\sigma_0^2 M_F(M_P-M_F)/M_P^2$$

to our data. Here M_P and M_F are the mass numbers of the projectile and fragment nuclei, respectively, and σ_0 is the fitted variable. In this fit, we assumed $M_F=2Z_F$ since the mass of fragments was not measured in our experiment. It should be noted that the final results change less than 15% if we take isotope production into account and use various possible A/Z ratios. The fit gives $\sigma_0=160$ MeV/c with χ^2 per degree of freedom of 2.4, which is compatible with the result of Greiner *et al.* at lower energies.[39]

Since much of the cross section for fragmentation at $14.5A$ GeV, at least for the Pb target, is due to electromagnetic dissociation, we infer from the above result that the momentum transfer in electromagnetic dissociation is not markedly different from that in nuclear spalla-

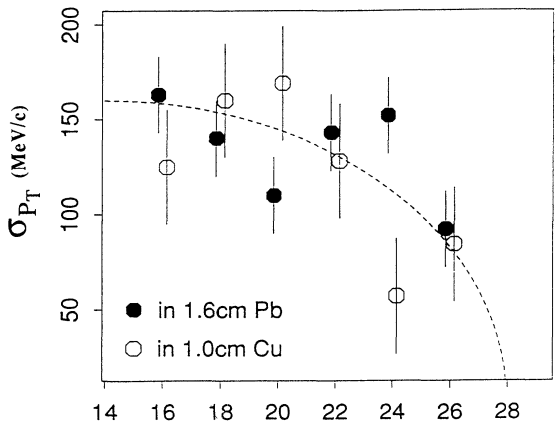

FIG. 12. Standard deviation in the transverse momentum distribution of projectile fragments produced in collisions of ^{28}Si nuclei with Pb (solid circles) and Cu (open circles). The parabolic fit to the data (dashed curve) gives $\sigma_0=160$ MeV/c.

tion. We can understand this similarity in terms of the following picture. In the fragmentation model the momentum transfer due to nuclear spallation is related to the Fermi motion of nucleons in the projectile nucleus by $\sigma_P^2 = 5\sigma_F^{2/3}$. In electromagnetic dissociation, the momentum due to the Coulomb collision is given by $P_T = 2Z_P Z_T e^2/bv$, where the impact parameter

$$b = 1.35(A_P^{1/3} + A_T^{1/3}) \text{ fm} .$$

The momentum transfers caused by these two processes are similar in order of magnitude. Moreover, if the electromagnetic dissociation occurs via the absorption of giant dipole resonances, the derived decay energy is in the possible region discussed in Ref. 51.

VI. CHARGE PICK-UP CROSS SECTION AT 14.5 A GeV

We followed ~75 000 Si nuclei in Pb and ~32 000 Si nuclei in Cu and found one *bona fide* charge pickup event. Charges measured at each surface of the stack of CR-39 detectors are shown in Fig. 13 for this event. We note that the event experienced a charge pickup reaction in the third Pb and interacted again in the first CR-39 sheet after the fourth Pb, losing one charge and returning to charge 14. The one-charge-loss reaction has a measured branching ratio of ~0.2 relative to the total charge-changing cross section of Si in Pb. Based on one event, we infer a charge pickup cross section of 0.07–1.3 mb for 14.5A GeV ^{28}Si in Pb at 68% confidence level. Based on a null result, we infer an upper limit of 0.9 mb for charge pickup in Cu at 68% confidence level.

At Bevalac energies, the charge pickup cross section has not been measured for a ^{28}Si beam. To investigate the energy dependence, we can either use an empirical

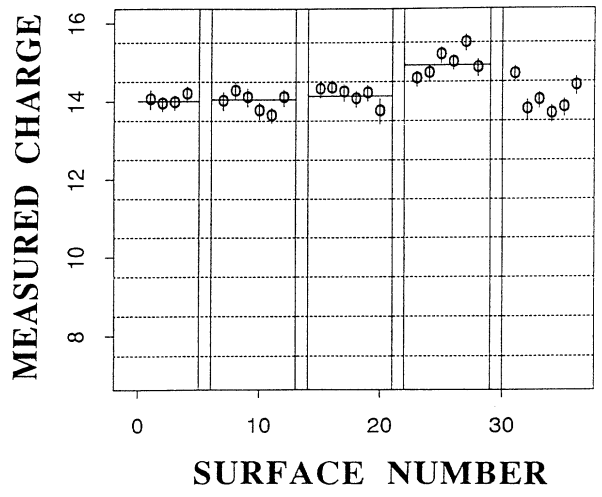

FIG. 13. One charge pickup event found in this experiment. The projectile experienced a charge pickup reaction in the third Pb target and then returned to charge $Z=14$ by losing one charge in the first CR-39 sheet after the fourth Pb target. In the plots, the surface number is accounted in such a way that it includes surfaces of target.

formula derived from data at Bevalac energies (Ref. 40) or simply interpolate logarithmically within data for a charge pickup of ^{12}C, ^{18}O, ^{20}Ne, ^{56}Fe, ^{84}Kr, ^{138}La, and ^{197}Au projectiles at Bevalac energies to get the cross section of ^{28}Si at ~1A GeV. In either case, the expected cross section at (1–2)A GeV is $\sigma_{\Delta Z=+1} = 0.1$–$0.7$ mb. The agreement between this estimate and our data leads to the interesting conclusion that there is essentially no energy dependence of the charge pickup cross section in the interval (1–14.5)A GeV.

The provocative conclusion by Ren *et al.*[40] that the charge pickup cross section at energies of ~(1–2)A GeV is proportional to A_P^2 has not yet led to a quantitative theoretical model. It would be interesting to extend measurements of charge pickup another order of magnitude higher in energy by using the ^{32}S beam at CERN.

VII. ADDITIONAL DISCUSSION

The interaction cross sections of secondary nuclei, and particularly the local interaction cross section as a function of distance from the creation point, have long been used to characterize whether secondary fragments show anomalous behavior. Two facts established in this experiment—a global enhancement of ~10% in total charge-changing cross section of secondary nuclei and a stringent limit on the dependence of local mean free path for charge-changing interaction on the distance from the point of origin—exclude anomalous fragments with the properties usually searched for ($f=5$–10%, $r=0.01$–0.1), but are consistent with a class of two-component models in which a large fraction of fragment nuclei has moderately enhanced interaction cross section. The values of f and r allowed in our experiment seem best accounted for in terms of production of weakly unstable isotopes. An acceptable fit to our data is obtained if ~30% of the fragments produced in reactions of primary nuclei are weakly unstable (and thus less tightly bound) isotopes with ~25% higher cross section than the stable (and most tightly bound) isotope. This conclusion does not necessarily imply new physics, but it does lead to the prediction that, when it becomes possible to identify the masses of fragment nuclei produced at 14.5A GeV, it will be found that their charge-loss cross sections are enhanced by ~25% over those of stable nuclei. Our experimental findings provide no support for the existence of "classical" anomalous fragments.

We observed that odd-Z fragments have higher charge-loss cross sections than even-Z fragments, which, in turn, have higher charge-loss cross sections than values predicted by an interpolation between values for ^{32}S and ^{16}O. This result could come about in either of two ways: (1) Primary (i.e., stable) odd-Z nuclei have substantially higher cross sections than their even-Z stable neighbors, in which case both even-Z and odd-Z unstable secondary nuclei have cross sections enhanced by similar amounts, of the order of 10%. (2) Both odd-Z and even-Z stable nuclei have charge-loss cross sections lying along an interpolation between values for ^{32}S and ^{16}O and odd-Z unstable secondary nuclei have charge-loss cross sections enhanced by at least twice as much as

even-Z unstable secondary nuclei.

Reviewing published studies of nuclear fragmentation cross sections at the Bevalac and at Dubna, which include the recent systematic measurements by Webber *et al.*,[52] we found no evidence for *large* enhancements of cross sections of secondary nuclei, with the exception of the studies of nearly unbound nuclides such as ^{11}Li and ^{14}Be. Of all the previous studies of secondary interactions, only the one by Symons *et al.*[20] had counting statistics sufficiently good to detect a weak odd-even effect. A careful inspection of their data shows that the charge-changing cross sections for odd-Z projectile fragments of 1.8A GeV Fe appear to be higher by 2–3 % than those for the even-Z neighbor at $Z=12$. Our new data seem to show that differences in charge-loss cross sections for odd-Z and even-Z nuclei are substantially larger at 14.5 than at (1–2)A GeV.

In the remainder of this section we comment on the relative roles played by electromagnetic and nuclear spallation in fragmentation at 14.5A GeV. A comparison of the data taken with the two stacks shows that both the Cu and the Pb targets create secondaries with similar properties, namely, that secondaries have enhanced charge-loss cross sections in a Pb target, whether they were created in a Cu or a Pb target, and do not have enhanced charge-loss cross sections in a Cu target. We know that electromagnetic spallation is more important in a Pb target than in a Cu target. We conclude that electromagnetic and nuclear spallation create the same types of secondaries, but that the increased frequency of interactions of these secondaries is mainly due to an increase in the electromagnetic spallation cross section. The much greater enhancement in charge-loss cross sections of odd-Z nuclei relative to even-Z nuclei at 14.5 than at 1–2A GeV, and for a Pb target rather than for a Cu target, suggests that the odd-even effect is stronger for electromagnetic spallation than for nuclear spallation.

Llope and Braun-Munzinger[53] have shown that recent data[49] on cross sections for a number of electromagnetic dissociation reactions of 14.5A GeV ^{28}Si are consistent with a model of first-order electromagnetic excitation followed by statistical decay of the excited nucleus. For eight reactions ranging from $1n$ to $2p2n$, they found an exponential decrease of exclusive cross section with negative-Q value, corresponding to a factor of 1.24 decrease per 1 MeV change in Q. As an example, they predict a 335-mb cross section for ^{28}Si breaking into ^{4}He+^{24}Mg, with $Q=-10$ MeV. Based on their exponential relation, we would expect increases of 15–25 % in the cross sections for alpha emission from ^{27}Si and ^{26}Si. Typically, in cases of secondary beams of interest in the present work, the Q values are 1 or 2 MeV less negative for charged-particle emission from off-stability isotopes than for their stable neighbors. This would imply increases by 25–55 % in cross sections for specific reactions. It would be interesting to use the model of Llope and Braun-Munzinger to make quantitative predictions of $\sigma_{\Delta Z}$ for off-stability projectiles.

We are currently engaged in a study of the behavior of nuclear fragments with charge $Z_F=6-15$ produced at CERN in interactions of a 200 GeV/nucleon ^{32}S beam with Cu and Pb targets.

ACKNOWLEDGMENTS

We thank Dana Beavis and the staff of the Brookhaven AGS accelerator for the ^{28}Si exposure, W. T. Williams for helpful discussions on data analysis, and M. Solarz for experimental assistance. This work was supported in part by the U.S. Department of Energy and by National Science Foundation Grant No. INT-8820389, which made it possible for Y.D. H. to work at Berkeley.

[1] P. B. Price, Ren Guoxiao, and W. T. Williams, Phys. Rev. Lett. **61**, 2193 (1988).
[2] C. Brechtmann and W. Heinrich, Z. Phys. A **330**, 407 (1988).
[3] C. Brechtmann and W. Heinrich, Z. Phys. A **331**, 463 (1988).
[4] C. Brechtmann, W. Heinrich, and E. V. Benton, Phys. Rev. C **39**, 2222 (1989).
[5] W. Mittig *et al.*, Phys. Rev. Lett. **59**, 1889 (1987).
[6] I. Tanihata, Nucl. Phys. **A488**, 113c (1988).
[7] I. Tanihata *et al.*, in *Treatise on Heavy-Ion Science,* edited by D. A. Bromley (Plenum, New York, 1989), Vol. 8, p. 443.
[8] P. G. Hansen and B. Jonson, Europhys. Lett. **4**, 409 (1989).
[9] For a review of anomalous nuclear fragments, see S. Fredriksson, G. Eilam, G. Berlad, and L. Bergstrom, Phys. Rep. **144**, 187 (1987).
[10] E. M. Friedlander *et al.*, Phys. Rev. Lett. **45**, 1084 (1980); Phys. Rev. C **28**, 1489 (1983).
[11] P. L. Jain and G. Das, Phys. Rev. Lett. **48**, 305 (1982).
[12] A. Milone, Nuovo Cimento Suppl. **12**, 353 (1954); S. Tokunaga, T. Ishii, and K. Nishikawa, Nuovo Cimento **5**, 517 (1957); H. Yagoda, *ibid.* **6**, 559 (1957); E. M. Friedlander and M. Spirchez, Nucl. Sci. Abstr. **15**, 3457 (1961); T. F. Cleghorn, P. S. Freier and C. J. Waddington, Can. J. Phys. Suppl. **46**, 572 (1968); B. Judek, Can. J. Phys. **46**, 343 (1968); **50**, 2080 (1972); H. Barber, P. S. Freier, and C. J. Waddington, Phys. Rev. Lett. **48**, 856 (1982).
[13] P. B. Price *et al.*, Phys. Rev. Lett. **50**, 556 (1982).
[14] M. L. Tincknell, P. B. Price, and S. P. Perlmutter, Phys. Rev. Lett. **51**, 1948 (1983).
[15] W. Heinrich *et al.*, Nucl. Phys. **A400**, 315c (1983).
[16] W. Heinrich *et al.*, Phys. Rev. Lett. **52**, 1401 (1984).
[17] H. Drechsel *et al.*, Phys. Rev. Lett. **54**, 30 (1985).
[18] H. Drechsel *et al.*, Phys. Rev. Lett. **55**, 1258 (1985).
[19] J. D. Stevenson, J. A. Musser, and S. W. Barwick, Phys. Rev. Lett. **52**, 515 (1984).
[20] T. J. M. Symons *et al.*, Phys. Rev. Lett. **52**, 982 (1984).
[21] T. M. Liss, S. P. Ahlen, P. B. Price, and G. Tarle, Phys. Rev. Lett. **49**, 775 (1982).
[22] H. A. Gustafsson *et al.*, Phys. Rev. Lett. **51**, 363 (1983).
[23] R. Holynski *et al.*, in *Proceedings 18th International Cosmic Ray Conference,* Bangalore, India, 1983, edited by N. Durgaprasad and P. V. Ramana Murthy (Tata Institute of Fundamental Research, Bombay, India, 1983), Vol. 11, p. 44.
[24] G. Baroni *et al.*, Nucl. Phys. **A437**, 729 (1985).
[25] R. Bhanja *et al.*, Phys. Rev. Lett. **54**, 771 (1985).

[26]A. Z. M. Ismail *et al.*, Phys. Rev. Lett. **52**, 1280 (1984).
[27]S. Beri *et al.*, Phys. Rev. Lett. **54**, 771 (1985).
[28]D. Ghosh *et al.*, *Proceedings 18th International Cosmic Ray Conference,* Bangalore, India, August 22 to September 3, 1983 (edited by N. Durgaprasad and P. V. Ramana Murthy (Tata Institute of Fundamental Research, Bombay, India, 1983), Vol. 5, p. 115.
[29]E. A. Alekseeva *et al.*, Pis'ma Zh. Eksp. Teor. Fiz. **38**, 411 (1983) [JETP Lett. **38**, 500 (1983)].
[30]A. A. Kartamyshev *et al.*, Pis'ma Zh. Eksp. Teor. Fiz. **40**, 313 (1984) [JETP Lett. **40**, 1105 (1984).
[31]M. El-Nadi *et al.*, Phys. Rev. Lett. **52**, 1971 (1984).
[32]P. L. Jain, M. M. Aggarwal, and K. L. Gomber, Phys. Rev. Lett. **52**, 2213 (1984).
[33]M. N. Agakishiev *et al.*, Z. Phys. C **16**, 307 (1983).
[34]R. L. Clarke *et al.*, Phys. Rev. D **27**, 2773 (1983).
[35]M. K. Sundaresan and P. J. S. Watson, Phys. Rev. D **27**, 2773 (1983).
[36]A. P. Gasparian and N. S. Grigalashvili, Z. Phys. A **320**, 459 (1985).
[37]A. G. Karev *et al.*, Yad. Fiz. **50**, 727 (1989) [Sov. J. Nucl. Phys. **50**, 452 (1989)].
[38]G. Gerbier, W. T. Williams, P. B. Price, and Ren Guoxiao, Phys. Rev. Lett. **59**, 2535 (1987).
[39]D. E. Greiner *et al.*, Phys. Rev. Lett. **35**, 152 (1975).
[40]Ren Guoxiao, P. B. Price, and W. T. Williams, Phys. Rev. C **39**, 1351 (1989).
[41]Jing Guiru, W. T. Williams, and P. B. Price, Phys. Rev. C **42**, 769 (1990).
[42]W. R. Binns *et al.*, Phys. Rev. C **39**, 1785 (1989); J. R. Cummings *et al.*, *ibid.* (in press).
[43]Y. D. He, P. B. Price, and W. T. Williams, Phys. Lett. B (in press).
[44]R. L. Fleischer, P. B. Price, and R. M. Walker, *Nuclear Tracks in Solids* (University of California Press, Berkeley, 1975).
[45]G. D. Westfall *et al.*, Phys. Rev. C **19**, 1309 (1979).
[46]P. J. Lindstrom, D. E. Greiner, and H. H. Heckman, Bull. Am. Phys. Soc. **17**, 488 (1972); H. H. Heckman, D. E. Greiner, P. J. Lindstrom, and H. Shwe, Phys. Rev. C **17**, 1735 (1978).
[47]P. J. Karol, Phys. Rev. C **11**, 1203 (1975).
[48]C. A. Bertulani and G. Baur, Phys. Rep. **163**, 299 (1988).
[49]J. Barrette *et al.*, Phys. Rev. C **41**, 1512 (1989).
[50]A. S. Goldhaber, Phys. Lett. **53B**, 306 (1974).
[51]G. Singh, K. Sengupta, and P. L. Jain, Phys. Rev. C **41**, 999 (1990).
[52]W. R. Webber, J. C. Kish, and D. A. Schrier, Phys. Rev. C **41**, 520 (1990).
[53]W. J. Llope and P. Braun-Munzinger, Phys. Rev. C **41**, 2644 (1990).